

Study on Controlling Brushless DC Motor in Current Control Loop Using DC-Link Current

Nguyen Thi Thanh Nga¹, Nguyen Thi Phuong Chi², Nguyen Hong Quang³

¹(Automation Department, Thai Nguyen University of Technology, Vietnam)

²(Automation Department, Thai Nguyen University of Technology, Vietnam)

³(Automation Department, Thai Nguyen University of Technology, Vietnam)

Corresponding Author: Nguyen Thi Thanh Nga

ABSTRACT : The Brushless DC motor (BLDC) has been being used widely due to high starting torque and the absence of brushes and commutators. As a result, BLDC motors have many advantages such as their high speed ranges, higher efficiency, better speed versus torque characteristics, long operating life and noiseless operation. However, these motors demand a complex design in control and power circuits. Basically, in order to implement the current control loop, it is necessary to measure current in at least 2 phases of 3 phases and use different variable-frequency pulse modulation methods such as current control with delay range algorithm. The paper proposes the design for Cascade Control system which has two control loops of speed and current. The pulse width modulation (PWM) speed control with fixed frequency is considered as appropriate to applications of microcontrollers. In current control loop, DC-link current acts as feedback signal, which enables to reduce the number of current sensors and be suitable for microcontrollers. The efficiency of the proposed controllers is demonstrated through a range of simulation results and experimental results for BLDC motors.

KEYWORDS - BLDC motor, cascade control, PWM, DC-Link, PI controller.

Date of Submission: 16-05-2018

Date of acceptance: 31-05-2018

I INTRODUCTION

Recently, the BLDC motors are used in many applications such as optical drives, radiator cooling fans of laptops, household appliances and office automation. In these applications, control circuits are designed simply and reliably. With the development of semiconductor switching technology and the design of high power converters, the performance of the electric drive systems using BLDC motors is better than that of others using DC motors as well as synchronous motors. Take mobile vehicles consuming independent DC voltage sources from batteries or solar energy as an example, especially drive systems of electric vehicles, cars and aircrafts with the capacity from several W to hundreds of kW.

There is a variety of proposed papers in terms of different speed control methods of BLDC motors. They work on tuning PID parameters as based on genetic algorithm, Ziegler Nicholas tuning methods and other work on adjusting PID parameters by fuzzy optimized algorithm or using fractional order PID controller [4-7]. The BLDC motor is non-linear and multi variable system due to temperature or load, so that it is difficult to drive it with accurate and reliable control response using the classical controlling methods.

The paper proposes a PI controller using for both current and speed control loops. The effective performance of the proposed controller is proved by simulation results and experimental results for BLDC motor systems.

II THE MATHEMATICAL MODEL OF THE BLDC MOTOR

The main parts of the system are shown in the figure 1, which consists of three-phase star-connected stator windings and permanent magnet rotor. The motor is driven by three-phase inverter with trigger signals

generated by the controller. It depends on rotor position sensors connected to the switches from Q₁ to Q₆ in order to drive the motor with stator currents corresponding with the back emfs.

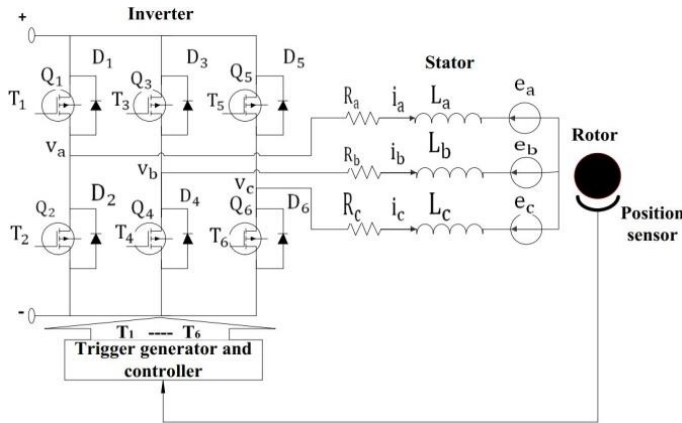


Fig. 1: The principle diagram of BLDC motor

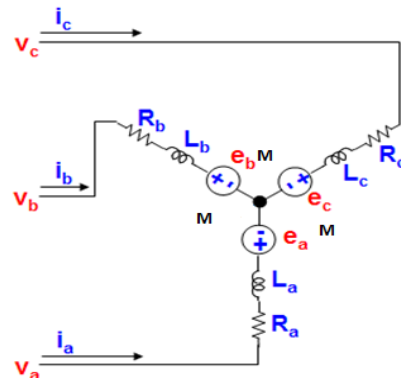


Fig. 2: The equivalent circuit diagram of three-phase voltages in BLDC motor

The stator phase voltages can be described by the following three equations (1):

$$\begin{aligned}
 V_a &= R_a i_a + L_a \frac{di_a}{dt} + M_{ab} \frac{di_b}{dt} + M_{ac} \frac{di_c}{dt} + e_a \\
 V_b &= R_b i_b + L_b \frac{di_b}{dt} + M_{ba} \frac{di_a}{dt} + M_{bc} \frac{di_c}{dt} + e_b \\
 V_c &= R_c i_c + L_c \frac{di_c}{dt} + M_{cb} \frac{di_b}{dt} + M_{ca} \frac{di_a}{dt} + e_c
 \end{aligned}
 \tag{1}$$

If three-phase system is balanced, we have:

$$R_a = R_b = R_c = R, L_a = L_b = L_c = L, M_{ab} = M_{ac} = M_{ba} = M_{bc} = M_{cb} = M_{ca} = M$$

Equations (1) become a set of equation (2)

$$\begin{aligned}
 V_a &= R i_a + L \frac{di_a}{dt} + M \frac{di_b}{dt} + M \frac{di_c}{dt} + e_a \\
 V_b &= R i_b + L \frac{di_b}{dt} + M \frac{di_a}{dt} + M \frac{di_c}{dt} + e_b \\
 V_c &= R i_c + L \frac{di_c}{dt} + M \frac{di_b}{dt} + M \frac{di_a}{dt} + e_c
 \end{aligned}
 \tag{2}$$

Transforming equations (2), we have:

$$\begin{aligned}
 v_a &= R i_a + (L - M) \frac{di_a}{dt} + e_a \\
 v_b &= R i_b + (L - M) \frac{di_b}{dt} + e_b \\
 v_c &= R i_c + (L - M) \frac{di_c}{dt} + e_c
 \end{aligned}
 \tag{3}$$

If neglecting mutual inductances then equations (3) are rearranged as:

$$\begin{aligned}
 v_a &= R i_a + L \frac{di_a}{dt} + e_a \\
 v_b &= R i_b + L \frac{di_b}{dt} + e_b \\
 v_c &= R i_c + L \frac{di_c}{dt} + e_c
 \end{aligned}
 \tag{4}$$

The electromagnetic torque is defined as (5), (6):

$$T_e = \frac{e_a i_a + e_b i_b + e_c i_c}{\omega_r} \tag{5}$$

The electromagnetic torque of motion for simple system is: $T_e = B_m \omega_r + J_m \frac{d}{dt} \omega_r + T_L$ (6)

where TL is the load torque, Jm is rotor inertial and B is friction constant.

III DESIGN THE PI CONTROLLER FOR SPEED AND CURRENT CONTROL

In this paper, the pulse width modulation (PWM) is used for this cascade control system with the current control loop inside and the speed control loop outside shown in figure 3.

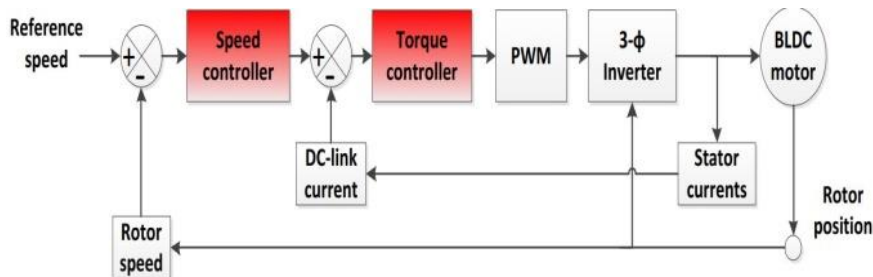


Fig. 3: The block diagram of proposed controllers for BLDC motor

The model of the command system contains a BLDC motor, inverter to three phase, pulsewidth modulation (PWM) and speed and current controllers. The BLDC motor speed can be directly changed by the duty cycle of the inverter switches in which firing signals depend on the control error. The control system consists of current sensors to measure three phase currents to obtain the DC-link current. Contemporarily, the rotor position sensors give the desired commutation sequence.

The speed controller is PI controller and has equation (7) as: $I_d = K_{P\omega}(\omega_d - \omega_f) + K_{I\omega} \int (\omega_d - \omega_f) dt$ (7)

In the speed control loop, the DC-link current is the control current due to it is also the three-phase currents and its sequence is chosen in table 1. When the system receives the phase current feedback, the phase voltage is calculated by equation (8): $V_d = K_{PI}(I_d - I) + K_{II} \int (I_d - I) dt$ (8)

Pole position and speed signals are determined through a set of Hall-effect sensors [2], [9]. Decoding and choosing phases are described as figure 4 and table 1.

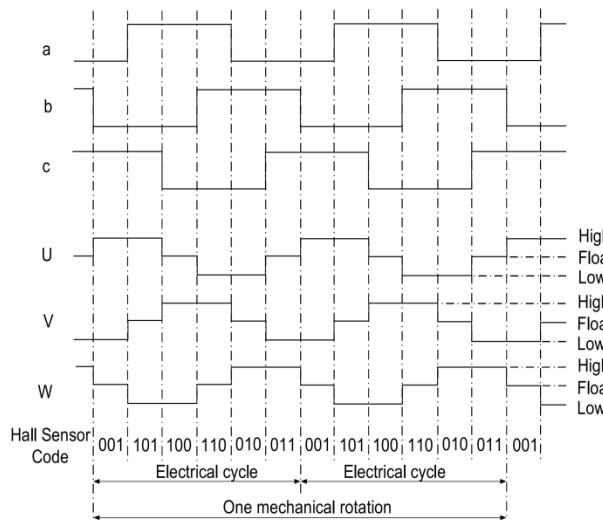


Fig. 4: The phase control rule based on Hall-effect sensors

Table 1: The selection of the DC-link phase current

Voltage vector	(S ₁ , S ₄)	(S ₃ , S ₆)	(S ₅ , S ₂)	Phase current
V ₁	(1,0)	(0,0)	(0,1)	i _a = i _{dc}
V ₂	(1,0)	(1,0)	(0,1)	i _c = -i _{dc}
V ₃	(0,1)	(1,0)	(0,0)	i _b = i _{dc}
V ₄	(0,1)	(0,0)	(1,0)	i _a = -i _{dc}
V ₅	(0,0)	(0,1)	(1,0)	i _c = i _{dc}
V ₆	(1,0)	(0,1)	(0,0)	i _b = -i _{dc}

Because the armature back emfs when controlling current are kept constant, the structure diagram of the system is shown equivalently as figure 5.

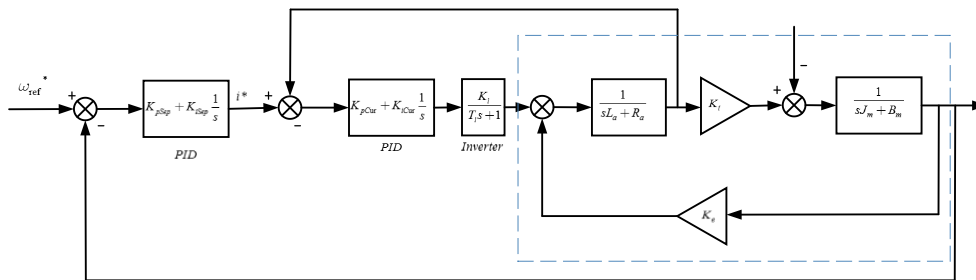


Fig. 5: The equivalent block diagram of the system with the DC-link feedback current

With the above structure, it is possible to apply different methods of linear control algorithms applied to DC motor. According to the PI controller of the current control as [1], [5], [6], [8], the dynamics of the measurement and the inverter circuit is considered lower than that of current. Then, the simple equivalent model of current control loop is depicted as figure 6.

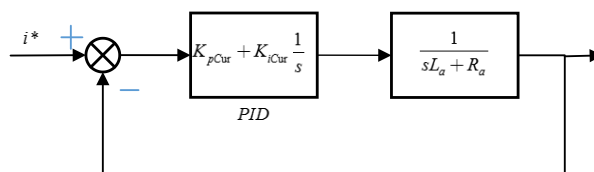


Fig. 6: The simple equivalent model of current control loop

The transfer function of the open loop from the model (6) is determined by equation (9):

$$G_h(s) = \frac{1}{s} \frac{K_{iCur} + K_{pCur}s}{R_a + L_a s} = \frac{K_{iCur}}{sR_a} \frac{1 + Ks}{1 + T_a s} \quad (9)$$

Controller parameters are selected based on the desired switching frequency of the closed system and reduced-order model as following: $\omega_{kCur} = \frac{K_{iCur}}{R_a}$, $\frac{K_{pCur}}{K_{iCur}} = \frac{L_a}{R_a}$

For the speed control loop, it is assumed that the current control loop is ideal, meaning that the transfer function of the closed current control loop is equal to 1. It is practicable since the dynamics of the current control loop is much faster than that of the speed control loop [2].

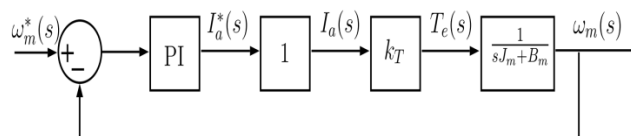


Fig. 7: The simple equivalent model of speed control loop

Similarly, the design of the speed controller is also based on the required switching frequency of the closed system and the reduced-order model as equation (9) with: $\omega_{kCur} = \frac{K_{iSpe} K_T}{B_m}$, $\frac{K_{pCur}}{K_{iCur}} = \frac{B_m}{J_m}$

IV SIMULATION AND EXPERIMENTAL RESULTS

In order to verify the performance of the control algorithm, the simulation and experimental methods are implemented for the BLDC motor with the following parameters as: $P_{rated} = 60W$; $p = 4$; $R_s = 2.08\Omega$; $L = 5.5$ mH; $J = 0.00019$ kg.m²; Simulating the cascade control method for the BLDC motor with the DC-link current feedback is shown as figure 8.

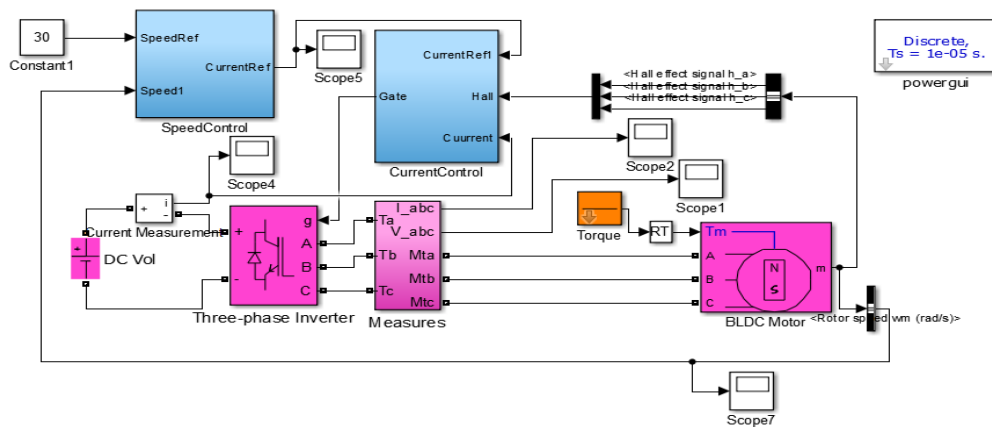


Fig. 8: The simulating model of the system in MATLAB/Simulink

Next, the distribution of different cases according to controller parameters is arranged in table 2.

Table 2: The controller parameters in the simulation

	K_p (speed controller)	K_i (speed controller)	K_p (current controller)	K_i (current controller)
Case 1	0.5	1	1.2	0.1
Case 2	0.2	0.5	1.2	0.1
Case 3	0.05	0.05	1.2	0.1
Case 4	0.2	0.5	0.5	0.01
Case 5	0.2	0.5	0.5	0.1
Case 6	0.2	0.5	2	0.1

The experimental module for the BLDC motor designed as figures 9 and 10 includes power source, a control card and an inverter board. The control card uses Dspic33FJ64MC506 microcontroller which thanks DSP block to implement control algorithms, PWM module to modulate pulse and 10-bit ADC at high speed about 1Mps.

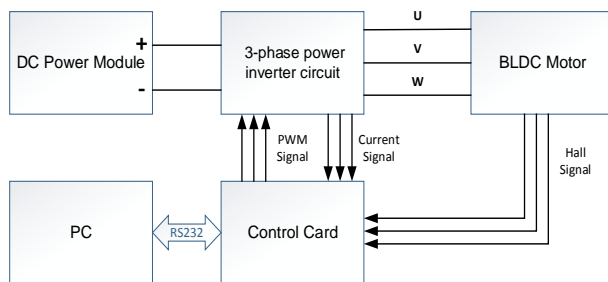


Fig. 9: The block diagram to control the BLDC motor

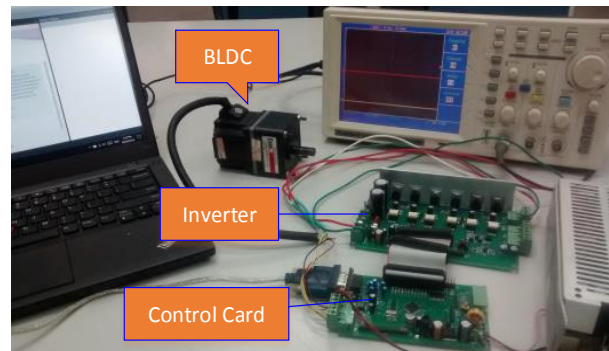


Fig. 10: The experimental module for the BLDC motor

The simulation result of phase currents shown in figure 11 is obtain with speed control loop as $K_p=0.2$, $K_i=0.5$ and current control loop as $K_p=1.2$, $K_i=0.1$. The speed response when appearing load torque $T_L = 0.5Nm$ at the third second and signals of Hall-effect sensors are depicted in figures 12 and 13.

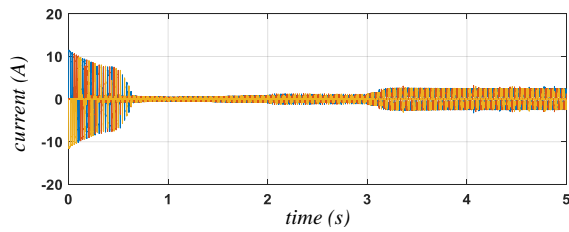


Fig. 11: The three-phase currents

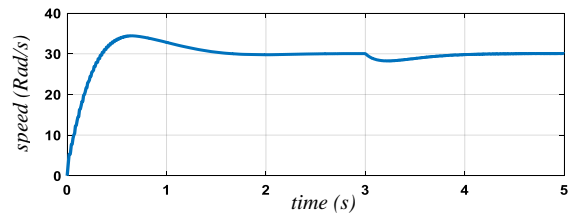


Fig. 12: The speed response with a load torque at the 3rd second

Speed and current responses gained by varying speed controller parameters and remaining current controller parameters in cases 1, 2 and 3 of table 2 are shown as figures 13 and 14, whereas figures 15 and 16 describe speed and current responses if remaining speed controller parameters and changing current controller parameters in cases 4, 5 and 6.

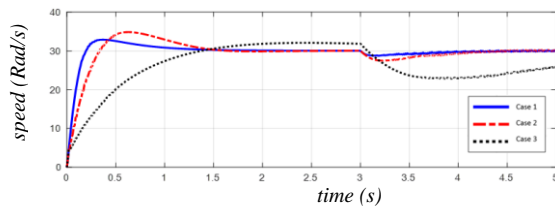


Fig. 13: The speed response with controller parameters in cases 1, 2 and 3

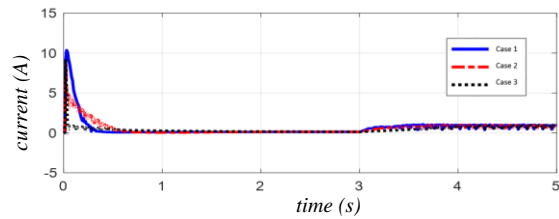


Fig. 14: The current response with controller parameters in cases 1, 2 and 3

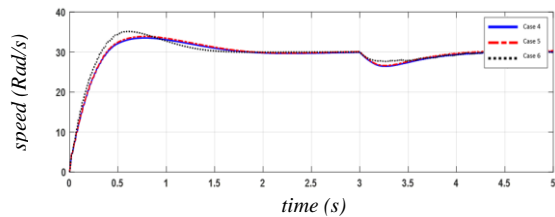


Fig. 15: The speed response with controller parameters in cases 4, 5 and 6

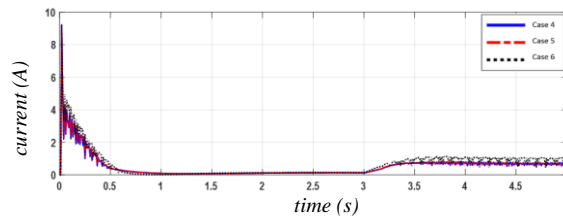


Fig. 16: The current response with controller parameters in cases 4, 5 and 6

The a-phase current is measured as starting the motor in figure 17 and the speed response when the speed reference reduces from 30 rad/s to 25 rad/s after 3 seconds, and then continues increasing to 30 rad/s within following 3 seconds is seen in figure 18.

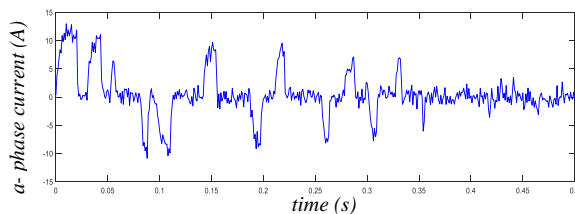


Fig. 17: The a-phase current

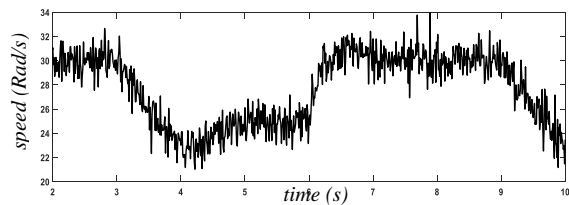


Fig. 18: The speed response if varying the speed reference

V CONCLUSION

The simulation and experimental results proved the effective performance of the proposed controller in tracking required speed references and preserving the stability of the system under the conditions of the load disturbance.

On the other hand, the cascade control algorithm with the inner current loop and the outer speed

loop gives expected results, responding to the different references in both simulation and experiments. Also, the use of the DC-link current is seen as completely practical, reducing the number of current sensors and simplifying the design and implementation of the controller.

VI ACKNOWLEDGMENTS

This research is funded by Thai Nguyen University of Technology under grant number T2018-B09.

REFERENCES

Journal Papers:

- [1]. Jun-Kyu Park and Jin Hur, Detection of Inter-Turn and Dynamic Eccentricity Faults Using Stator Current Frequency Pattern in IPM-Type BLDC Motors, *IEEE Trans. Ind. Electron.*, 63(3), March 2016.
- [2]. Pooya Alaeinovin and Juri Jatskevich, Filtering of Hall-Sensor Signals for Improved Operation of Brushless DC Motors, *IEEE Trans. Energy Convers.*, 27(2), Jun 2012.
- [3]. Jun-Kyu Park, Thusitha Randima Wellawatta, Zia Ullah, and Jin Hur, New Equivalent Circuit of the IPM-Type BLDC Motor for Calculation of Shaft Voltage by Considering Electric and Magnetic Fields, *IEEE Trans. Ind. App.*, 52(5), Sep/Oct 2016.
- [4]. Yong Liu, Student Member, IEEE, Z. Q. Zhu, Senior Member, IEEE, and David Howe, Direct Torque Control of Brushless DC Drives With Reduced Torque Ripple, *IEEE Transactions on Industry Applications*, 41(2), March/April 2005.
- [5]. Adel A. El-samahy, Mohamed A. Shamseldin, Brushless DC motor tracking control using self-tuning fuzzy PID control and model reference adaptive control, *Ain shams engineering Journal*, 2016.
- [6]. Hans Butler, GerHonderd, and Job van Amerongen, Model Reference Adaptive Control of a Direct-Drive DC Motor, *IEEE Control Systems Magazine*, 0'272-170818910100-0080, 1989.
- [7]. Salih Baris Ozturk Hamid A. Toliyat, Direct Torque Control of Brushless DC Motor with Non-sinusoidal Back-EMF, 1-4244-0743-5, 2007.

Books:

- [8]. Taha Nurettin Gucin, Muhammet Biberoglu, Bekir Fincan, Mehmet Onur Gulbahc, *Tuning Cascade PI(D) Controllers in PMDC Motor Drives: A Performance Comparison for Different Types of Tuning Methods*.
- [9]. José Carlos Gamazo-Real, Ernesto Vázquez-Sánchez and Jaime Gómez-Gi, *Position and Speed Control of Brushless DC Motors Using Sensorless Techniques and Application Trends*, 2010.

Nguyen Thi Thanh Nga." Study on Controlling Brushless DC Motor in Current Control Loop Using DC-Link Current" American Journal Of Engineering Research (AJER), Vol. 7, No. 5, 2018, Pp.522-528.